Mathematics and Computers in Simulation 34 (1992) 141–161
North-Holland

MATCOM 910

Analysis of finite elements and finite differences for shallow water equations: A review

B. Neta

Department of Mathematics, Naval Postgraduate School, Monterey, CA 93943, United States

Abstract

Neta, B., Analysis of finite elements and finite differences for shallow water equations: A review, Mathematics and Computers in Simulation 34 (1992) 141–161.

In this review article we discuss analyses of finite-element and finite-difference approximations of the shallow water equations. An extensive bibliography is given.

0. Introduction

In this article we review analyses of finite-element and finite-difference methods for the approximation of the shallow water equations. Results by the author and others are given, tables showing side by side all these results are included. Current research including semi-Lagrangian and domain decomposition methods are covered. An extensive bibliography is given.

1. Shallow water equations

1.1. Model

Consider a sheet of fluid with constant and uniform density (see, for example, [41]). (See Fig. 1.) The height of the surface of the fluid above the reference level $z = 0$ is $h(x, y, t)$. With atmosphere or ocean in mind, we model the body force arising from the potential $\phi = gh$. The rigid bottom is defined by the surface $z = h_B(x, y)$. The velocity has components u, v and w in the x-, y- and z-directions, respectively. The pressure of the fluid surface can be arbitrarily imposed, but here we assume it is constant. The fluid is assumed *inviscid*, that is, only motions for which viscosity is unimportant are considered.

Let H be the average depth of the fluid, $h - h_B$. Let L be a characteristic horizontal scale for the motion. For shallow water theory one must have

$$\frac{H}{L} \ll 1. \tag{1.1}$$

Correspondence to: Prof. B. Neta, Code MA/Nd, Department of Mathematics, Naval Postgraduate School, Monterey, CA 93943-5100, United States.

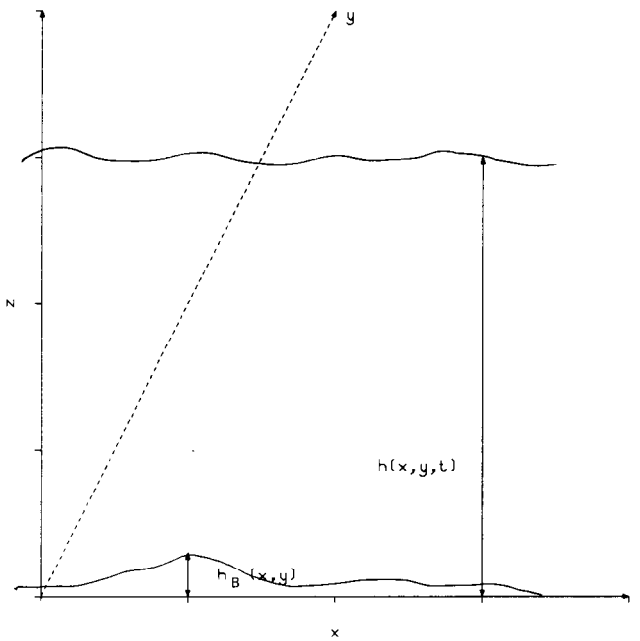

Fig. 1.

The shallow water model thus contains some of the important dynamical features of the atmosphere and ocean. The major physical deficiency is the absence of density stratification present in the real atmosphere and oceans.

1.2. Equations

The specification of incompressibility and constant density decouples the dynamics from the thermodynamics (see, e.g., [41]). The equation of *mass conservation* reduces to the condition of incompressibility:

$$\frac{\partial u}{\partial x}+\frac{\partial v}{\partial y}+\frac{\partial w}{\partial z}=0.$$

The momentum equations:

$$\begin{aligned}
&\frac{\partial u}{\partial t}+u\frac{\partial u}{\partial x}+v\frac{\partial u}{\partial y}+w\frac{\partial u}{\partial z}-fv=-\frac{1}{\rho}\frac{\partial \tilde{p}}{\partial x},\\
&\frac{\partial v}{\partial t}+u\frac{\partial v}{\partial x}+v\frac{\partial v}{\partial y}+w\frac{\partial v}{\partial z}+fu=-\frac{1}{\rho}\frac{\partial \tilde{p}}{\partial y},\\
&\frac{\partial w}{\partial t}+u\frac{\partial w}{\partial x}+v\frac{\partial w}{\partial y}+w\frac{\partial w}{\partial z}=-\frac{1}{\rho}\frac{\partial \tilde{p}}{\partial z},
\end{aligned} \tag{1.2}$$

where the total pressure $p(x, y, z, t)$ is

$$p(x, y, z, t) = -\rho g z + \tilde{p}(x, y, z, t). \tag{1.3}$$

Note that the horizontal pressure gradient is independent of z if one uses the hydrostatic approximation

$$\frac{\partial p}{\partial z} = -\rho g + \mathrm{O}\left(\left(\frac{H}{L}\right)^2\right). \tag{1.4}$$

Such approximation follows from scale analysis of the momentum equations and the incompressibility condition. Integrating the last equation and using the boundary condition

$$p(x, y, h) = p_0 \tag{1.5}$$

yields

$$p = \rho g(h - z) + p_0. \tag{1.6}$$

This means that the pressure in excess of p_0 at any point simply equals the weight of the unit column of fluid above the point at that time.

Note that the *horizontal pressure gradient* is independent of z, therefore the horizontal accelerations must be independent of z. For low Rossby-wave number $U/(fL)$, the Taylor–Proudman theorem (see, e.g., [41, p. 43]) applied to a homogeneous fluid will *require* the velocities to be independent of z.

The vertical momentum equation can be integrated easily, since u and v are independent of z,

$$w(x, y, z, t) = -z\left(\frac{\partial u}{\partial x} + \frac{\partial v}{\partial y}\right) + \tilde{w}(x, y, t). \tag{1.7}$$

The condition of *no* normal flow at the bottom requires

$$w(x, y, h_B, t) = u\frac{\partial h_B}{\partial x} + v\frac{\partial h_B}{\partial y}. \tag{1.8}$$

This leads to

$$w(x, y, z, t) = (h_B - z)\left(\frac{\partial u}{\partial x} + \frac{\partial v}{\partial y}\right) + u\frac{\partial h_B}{\partial x} + v\frac{\partial h_B}{\partial y}. \tag{1.9}$$

The corresponding kinematic condition at the surface $z = h$ is

$$w(x, y, z, t) = \frac{\partial h}{\partial t} + u\frac{\partial h}{\partial x} + v\frac{\partial h}{\partial y}. \tag{1.10}$$

Thus

$$\frac{\partial h}{\partial t} + \frac{\partial}{\partial x}[u(h - h_B)] + \frac{\partial}{\partial y}[v(h - h_B)] = 0. \tag{1.11}$$

This equation, combined with the horizontal momentum equations

$$\frac{\partial u}{\partial t} + u\frac{\partial u}{\partial x} + v\frac{\partial u}{\partial y} - fv = -g\frac{\partial h}{\partial x}, \qquad \frac{\partial v}{\partial t} + u\frac{\partial v}{\partial x} + v\frac{\partial v}{\partial y} + fu = -g\frac{\partial h}{\partial y} \tag{1.12}$$

form the shallow water equations.

Remarks. (1) The vertical momentum equation can be interpreted as follows: if the local horizontal divergence of volume $\nabla \cdot (\vec{u}H)$ is positive, it must be balanced by a local decrease of the layer thickness due to a drop in the free surface. Here we define the total depth $H = h - h_B$.

(2) The time it takes a fluid element to move a distance L with speed U is L/U. If that period of time is much less than the period of rotation of the earth, the fluid can barely feel the earth's rotation. For rotation to be important, we anticipate $U/(fL) \leqslant 1$. This ratio is called *Rossby number*.

2. Advection equation

Advective processes are dominant in atmospheric and oceanic circulation systems, while diffusive effects are important only in boundary layer regions. Any numerical model for these circulation systems should treat advective effects accurately. Neta and Williams [36] have analyzed various finite-element formulations of the linearized advection equation in two dimensions,

$$\frac{\partial F}{\partial t} + V\cos\theta\frac{\partial F}{\partial x} + V\sin\theta\frac{\partial F}{\partial y} = 0, \tag{2.1}$$

where V is the mean flow speed and θ is the direction relative to the x-axis. The analytic solution to (2.1) is

$$F(x, y, t) = F(x - tV\cos\theta, y - tV\sin\theta, 0). \tag{2.2}$$

The following methods were analyzed:

(i) linear elements on isosceles triangles;
(ii) linear elements on biased triangles;
(iii) linear elements on criss-cross grid;
(iv) linear elements on unbiased triangles;
(v) bilinear basis functions on rectangles;
(vi) second-order finite differences; and
(vii) fourth-order finite differences.

Figures 2–5 show various triangulations in the case $\Delta x = \Delta y$.

The leapfrog time differencing is used in all cases. For the case $\theta = 0$ (flow in the x-axis direction) one can show that if the initial condition is

$$F(x, y, 0) = K\,e^{i(kx+ly)}, \tag{2.3}$$

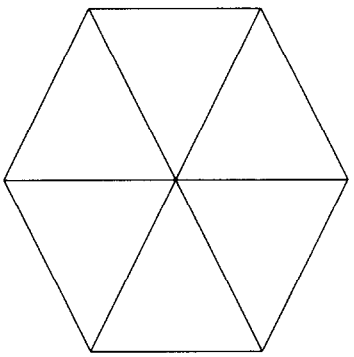

Fig. 2. Isosceles triangles.

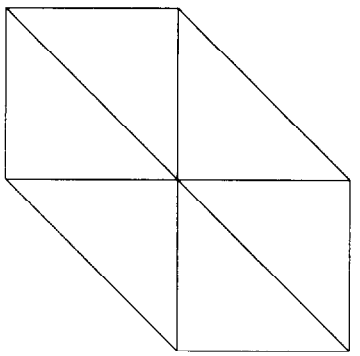

Fig. 3. Biased grid.

then the analytic solution is

$$F(x, y, t) = K\ \mathrm{e}^{\mathrm{i}(kx+ly-kVt)}. \tag{2.4}$$

Because of the localized nature of the schemes we obtained in each case an ordinary differential equation or a system of two such equations. The solution in each case is a wave

$$F(x, y, t) = A(t)\ \mathrm{e}^{\mathrm{i}(kx+ly)}. \tag{2.5}$$

The amplitude $A(t)$ can be solved in terms of σ (see Table 1 of functions σ for each scheme). The phase speed of the numerical solution is related to σ by

$$C_F = \frac{\arcsin\ \sigma}{k\ \Delta t}. \tag{2.6}$$

The use of leapfrog (centered difference) in time leads to a numerical solution consisting of two waves or modes. The spurious (computational) mode is damped. The CFL condition for stability of each scheme is given in Table 2.

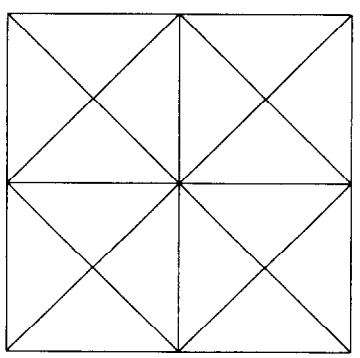

Fig. 4. Criss-cross grid.

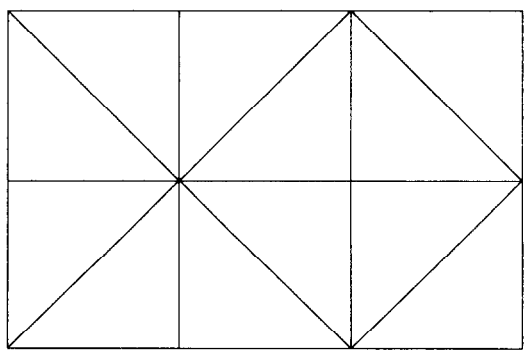

Fig. 5. Unbiased grid.

Table 1

	σ (for $\theta = 0$)
Isosceles	$4V\frac{\Delta t}{\Delta x}\frac{\sin k\,\Delta x + \sin \frac{1}{2}k\,\Delta x \cos l\,\Delta y}{3+\sin k\,\Delta x + 2\cos \frac{1}{2}k\,\Delta x \cos l\,\Delta y}$
Biased	$4V\frac{\Delta t}{d}\frac{\sin kd + \frac{1}{2}\sin ld + \frac{1}{2}\sin(k-l)d}{3+\cos kd + \cos ld + \cos(k-l)d}$, $\Delta x = \Delta y = \mathrm{d}$
Criss-cross	$2V\frac{\Delta t}{d}\frac{-b \pm \sqrt{b^2-4ae}}{2a}$, where $a = 4+\cos kd + \cos ld - \cos kd \cos \frac{1}{2}kd \cos ld \cos \frac{1}{2}ld$, $b = \sin kd - \sin \frac{3}{2}kd \cos ld \cos \frac{1}{2}ld$, $e = -\sin kd \sin \frac{1}{2}kd \cos ld \cos \frac{1}{2}ld$
Unbiased	$4V\frac{\Delta t}{d}\frac{\sin kd\left(\cos kd \pm \sqrt{q}\right)}{q-\cos^2 kd}$, where $q = 8+2\cos kd \cos ld - \cos^2 ld$
Rectangles	$3V\frac{\Delta t}{\Delta x}\frac{\sin k\,\Delta x}{2+\cos k\Delta x}$
Second-order finite differences	$V\frac{\Delta t}{\Delta x}\sin k\,\Delta x$
Fourth-order finite differences	$V\frac{\Delta t}{\Delta x}(\frac{4}{3}\sin k\Delta x - \frac{1}{6}\sin 2k\,\Delta x)$

Two of the schemes require special consideration. The criss-cross is unstable. The unbiased scheme has four modes like the criss-cross instead of two modes for the other methods. These two extra modes can explain the noise in the numerical solution experienced in [19].

The scheme with isosceles triangles is superior to all of the schemes which use right triangles. The rectangles become superior for larger y wave numbers. The finite-difference methods are both inferior to the stable finite elements.

For the general case $\theta \neq 0$, only isosceles triangles, biased triangles and bilinear rectangular elements are compared to the finite differences (see [36] for details and contour plots of C_F/C). (See Table 3.) The study concludes that both finite elements are superior to the finite

Table 2

	CFL condition $V\,\Delta t/\Delta x \leqslant$
Isosceles	0.45144
Biased	0.456
Rectangles	$1/\sqrt{3}$
Second-order finite differences	1
Fourth-order finite differences	0.73
Unbiased	0.5623

Table 3

σ (for $\theta \neq 0$)	
Isosceles (base angle θ)	$4V\cos\theta\dfrac{\Delta t}{\Delta x}\dfrac{3\cos\frac{1}{2}k\,\Delta x\sin l\,\Delta y+\sin k\,\Delta x+\sin\frac{1}{2}k\,\Delta x\cos l\,\Delta y}{3+\cos k\,\Delta x+2\cos\frac{1}{2}k\,\Delta x\cos l\,\Delta y}$
Rectangles (θ = angle between base and diagonal)	$3V\cos\theta\dfrac{\Delta t}{\Delta x}\left[\dfrac{\sin k\,\Delta x}{2+\cos k\,\Delta x}+\dfrac{\sin l\,\Delta y}{2+\cos l\,\Delta y}\right]$
Second-order finite differences	$V\cos\theta\dfrac{\Delta t}{\Delta x}(\sin k\,\Delta x+\sin l\,\Delta y)$
Fourth-order finite differences	$V\cos\theta\dfrac{\Delta t}{\Delta x}\left[\frac{4}{3}(\sin k\,\Delta x+\sin l\,\Delta y)-\frac{1}{6}(\sin 2k\,\Delta x+\sin 2l\,\Delta y)\right]$

difference. The triangles may lose their attractiveness if the resolution varies or the east–west boundary conditions are not periodic. Staniforth [52] discussed the efficiency of solution of finite-element scheme using rectangles.

3. Phase speed and group velocities for various schemes to solve the shallow water equation

The comparative study of the last section is continued both analytically and numerically in [39] for the shallow water equations with topography. The primitive formulation (Section 2) and the vorticity-divergence form are used. Cullen and Hall [9] showed that the accuracy of the Galerkin finite-element solution was better for the vorticity-divergence formulation than for an increase in resolution with the primitive formulation. Williams and Schoenstadt [67] noted that staggered variable formulation of the primitive equations and the unstaggered vorticity-divergence formulation gave the best treatment of geostrophic adjustment for small scale features.

The linearized shallow water equations in primitive form are

$$\begin{aligned}
&\frac{\partial u}{\partial t}+U\frac{\partial u}{\partial x}+V\frac{\partial u}{\partial y}-fv+g\frac{\partial h}{\partial x}=0,\\
&\frac{\partial v}{\partial t}+U\frac{\partial v}{\partial x}+V\frac{\partial v}{\partial y}+fv+g\frac{\partial h}{\partial y}=0,\\
&\frac{\partial h}{\partial t}+U\frac{\partial h}{\partial x}+V\frac{\partial h}{\partial y}+\gamma\left(\frac{\partial u}{\partial x}+\frac{\partial v}{\partial y}\right)=u\frac{\partial\gamma}{\partial x}+v\frac{\partial\gamma}{\partial y},
\end{aligned}\tag{3.1}$$

where U, V are the horizontal mean velocities and $\gamma=(H-h_B)$. The vorticity-divergence

formulation is obtained from the above when recalling that the vorticity ζ and divergence D are defined by

$$\zeta = \frac{\partial v}{\partial x} - \frac{\partial u}{\partial y}, \qquad D = \frac{\partial u}{\partial x} + \frac{\partial v}{\partial y}. \tag{3.2}$$

These equations are

$$\begin{aligned} &\frac{\partial h}{\partial t} + U\frac{\partial h}{\partial x} + V\frac{\partial h}{\partial y} + \gamma D = u\frac{\partial \gamma}{\partial x} + v\frac{\partial \gamma}{\partial y}, \\ &\frac{\partial \zeta}{\partial t} + U\frac{\partial \zeta}{\partial x} + V\frac{\partial \zeta}{\partial y} + fD = 0, \\ &f\zeta = g\,\nabla^2 h, \end{aligned} \tag{3.3}$$

with the geostrophic relations

$$fu = -g\frac{\partial h}{\partial y}, \qquad fv = g\frac{\partial h}{\partial x}. \tag{3.4}$$

The phase speed is

$$\frac{\sigma}{k} = \frac{1}{k}\left(kU + lV + \frac{(f/\gamma)(k\,\partial\gamma/\partial y - l\,\partial\gamma/\partial x)}{k^2 + l^2 + f^2/\gamma}\right). \tag{3.5}$$

The phase speed for the numerical methods discussed previously is given by

$$C_F = \frac{1}{k}\left(\frac{\psi}{\alpha}U + \frac{\beta}{\alpha}V + \frac{(f/\gamma)\left(\psi\dfrac{\partial\gamma}{\partial y} - \beta\dfrac{\partial\gamma}{\partial x}\right)}{\delta + \epsilon + f^2/\gamma}\right), \tag{3.6}$$

where α, β, ψ, δ, ϵ for each scheme are listed in Table 4. The group velocities are defined by the partial derivatives of the phase speed with respect to each of the wave numbers.

As discussed in Section 1, the distortion of the output (solution) depends on the transfer function. In the next section we discuss the use of transfer functions to analyze the shallow water equations.

4. Transfer functions

Linear (space *or* time) invariant systems can be described by the so-called transfer functions (see [58]). Let $y_i(x)$, $y_0(x)$ be the input and output to a system, respectively. Let $\hat{y}_i(k)$, $\hat{y}_0(k)$ be the Fourier transforms of the input and output, respectively, where

$$\hat{f}(k) = \int_{-\infty}^{\infty} f(x)\,\mathrm{e}^{-\mathrm{i}kx}\,\mathrm{d}x. \tag{4.1}$$

Table 4

	Isosceles	Rectangles	Second order	Fourth order
α	$(3+\cos k\,\Delta x+2\cos \frac{1}{2}k\,\Delta x\cos l\,\Delta y)\frac{1}{6}\Delta x\,\Delta y$	$(2+\cos k\Delta x)(2+\cos l\,\Delta y)\frac{1}{3}\Delta x\,\Delta y$	1	1
β	$(\Delta x)^2\cos \frac{1}{2}k\,\Delta x\sin l\,\Delta y$	$\frac{1}{3}(\Delta x)^2\sin l\,\Delta y\,(2+\cos k\,\Delta x)$	$\dfrac{\sin l\,\Delta y}{\Delta y}$	$\dfrac{4}{3}\dfrac{\sin l\,\Delta y}{\Delta y}-\dfrac{1}{6}\dfrac{\sin 2l\,\Delta y}{\Delta y}$
ψ	$\frac{4}{9}(\Delta y)^2(\sin k\,\Delta x+\sin \frac{1}{2}k\,\Delta x\cos l\,\Delta y)$	$\frac{1}{3}(\Delta y)^2\sin k\,\Delta x\,(2+\cos l\,\Delta y)$	$\dfrac{\sin k\,\Delta x}{\Delta x}$	$\dfrac{4}{3}\dfrac{\sin k\,\Delta x}{\Delta x}-\dfrac{1}{6}\dfrac{\sin 2k\,\Delta x}{\Delta x}$
δ	$2\dfrac{\Delta y}{\Delta x}(1-\cos k\,\Delta x)$	$2\dfrac{\Delta y}{\Delta x}(2+\cos l\,\Delta y)(1-\cos k\,\Delta x)$	$\dfrac{2}{(\Delta x)^2}(\cos k\,\Delta x-1)$	$-\dfrac{\cos 2k\,\Delta x-16\cos k\,\Delta x+15}{6(\Delta x)^2}$
ϵ	$\dfrac{1}{2}\dfrac{\Delta x}{\Delta y}(3+\cos k\,\Delta x-4\cos \frac{1}{2}k\,\Delta x\cos l\,\Delta y)$	$2\dfrac{\Delta x}{\Delta y}(2+\cos k\,\Delta x)(1-\cos l\,\Delta y)$	$\dfrac{2}{(\Delta y)^2}(\cos l\,\Delta y-1)$	$-\dfrac{\cos 2l\,\Delta y-16\cos l\,\Delta y+15}{6(\Delta y)^2}$

Then the Fourier transforms of the input and output are related by

$$\hat{y}_0(k) = \hat{\phi}(k)\hat{y}_i(k). \tag{4.2}$$

This is the representation of the system in the *transform domain*. The representation in the *physical domain* is given by the convolution theorem

$$y_0(x) = \int_{-\infty}^{\infty} \phi(x-r)y_i(r)\,\mathrm{d}r. \tag{4.3}$$

$\phi(x)$ is known as *impulse response* of the system to an input $\delta(x)$, since

$$\phi(x) = \int_{-\infty}^{\infty} \phi(x-r)\delta(r)\,\mathrm{d}r. \tag{4.4}$$

The magnitude and phase of $\hat{\phi}(k)$ can be found by taking a sinusoidal input

$$y_i(x) = \mathrm{e}^{\mathrm{j}k_i x}, \tag{4.5}$$

where $\mathrm{j} = \sqrt{-1}$. Then

$$y_0(x) = \hat{\phi}(k_i)\,\mathrm{e}^{\mathrm{j}k_i x} = |\hat{\phi}(k_i)|\,\mathrm{e}^{\mathrm{j}k_\phi}\,\mathrm{e}^{\mathrm{j}k_i x} = |\hat{\phi}(k_i)|\,\mathrm{e}^{\mathrm{j}k_i(x+k_\phi/k_i)}. \tag{4.6}$$

Thus, the magnitude $|\hat{\phi}|$ of the transfer function is the *factor* by which the amplitude of a *sinusoidal* is amplified or attenuated. The argument k_ϕ/k_i is the *shift* of the phase of the *input*.

In general, the different frequencies are amplified/attenuated and shifted in phase by different amounts. The *distortion* (change in shape) of the output depends on *both* effects.

In electrical engineering, any linear invariant system which can be described by a transfer function is called a *filter*. When a continuous process is discretized, one obtains a *discrete* or *digital filter*.

For example,

$$\frac{\mathrm{d}y}{\mathrm{d}x} = f(x), \tag{4.7}$$

where $f(x)$ is input and $y(x)$ is output, is a filter. A digital filter for this could be

$$y(x+\Delta x) = y(x) + \Delta x\, f(x) \tag{4.8}$$

(nothing more than Euler's method). The transfer function of digital filters can be determined by Fourier transform. To this end, one recalls

$$\hat{y}(x+\Delta x) = \int_{-\infty}^{\infty} y(x+\Delta x)\,\mathrm{e}^{-\mathrm{j}kx}\,\mathrm{d}x = \mathrm{e}^{\mathrm{j}k\,\Delta x}\hat{y}(x). \tag{4.9}$$

The transfer function for the filter is

$$\hat{\phi}(k) = \frac{1}{\mathrm{j}k}, \tag{4.10}$$

and for the above digital filter is (easy exercise)

$$\hat{\phi}(k) = \frac{e^{-jk\,\Delta x/2}}{j\dfrac{\sin \frac{1}{2}k\ \Delta x}{\frac{1}{2}\Delta x}}. \tag{4.11}$$

The main difference between continuous and digital filters is the so-called *aliasing*. A sampling device at interval Δx is *not* capable of resolving waves of frequency greater than $\pi/\Delta x$ and if energy is present in a sampled continuous signal at such high frequencies, it will erroneously be resolved into a frequency lower than π/Δx.

5. Transfer function analysis for one-dimensional shallow water equations

5.1. Analytic case

The one-dimensional linearized shallow water equations with no mean flow were analyzed in [48]:

$$\frac{\partial u}{\partial t} - fv + g\frac{\partial h}{\partial x} = 0, \qquad \frac{\partial v}{\partial t} + fu = 0, \qquad \frac{\partial h}{\partial t} + H\frac{\partial u}{\partial x} = 0. \tag{5.1}$$

This model is especially important in the study of geostrophic adjustment. This process has been studied in some detail from several approaches in [1–3,45,47,69]. The process of geostrophic adjustment is important because it is the primary mechanism by which the atmosphere reacts to errors in the initial data. The process takes place by means of wave propagation from local regions of initial imbalance, leaving behind a steady semigeostrophic balance flow. Cahn [3] showed that a sudden perturbation caused by an addition of momentum will cause the disturbance amplitude to first grow linearly with time followed by an asymptotic state

$$gh \sim \frac{1}{\sqrt{ft}}\cos\left(ft + \tfrac{1}{4}\pi\right). \tag{5.2}$$

The speed of propagation of energy is $\sqrt{gh}$. Obukhov [40] showed that for two-dimensional flow

$$gh \sim \mathrm{O}\left(\frac{1}{t}\right). \tag{5.3}$$

Schoenstadt [48] has shown that the amplitude distortion in this system is governed by one of the three factors $1/\nu$, k/σ or k/ν^2, or the square of one of these were ν/k, the phase speed, is given by

$$\frac{\nu}{k} = \frac{f}{k}\sqrt{1 + R_0^2 k^2}, \tag{5.4}$$

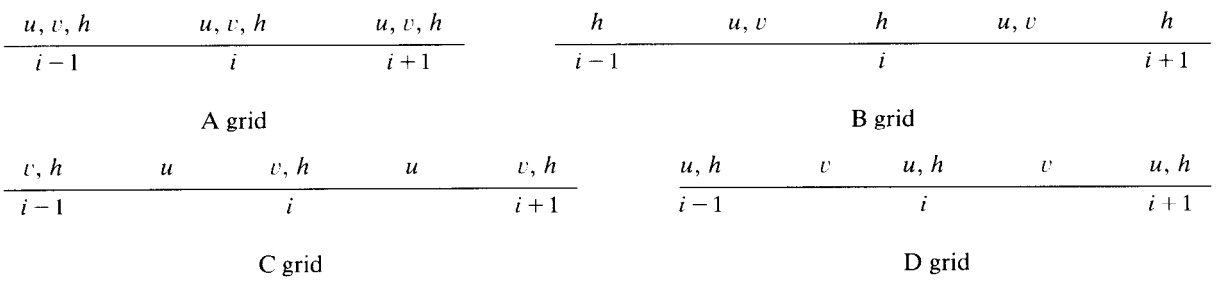

Fig. 6.

where

$$R_0 = \frac{\sqrt{gH}}{f} \tag{5.5}$$

is the Rossby radius of deformation.

When drawing the amplitude coefficients, it is clear that the terms with the coefficient $1/\nu$ have their low frequencies least affected (low-pass filter), the terms with coefficient k/ν are high-pass filters and those with k/ν^2 are band-pass filters.

5.2. *Semi-discrete case*

Schoenstadt [48] analyzed second- and fourth-order finite-difference and finite-element schemes for which the variables are either unstaggered (A grid) or staggered (B, C, D grids) (see Fig. 6). Finite-element D grid is not given there. See also [25].

Neta and Navon [34] analyzed the Turkel–Zwas explicit large time step scheme [61]. The filter coefficients $1/\nu$, k/ν, k/ν^2 are replaced, respectively, by τ/ν, S/ν, $\tau S/\nu^2$. For the Turkel–Zwas scheme the filter coefficients change but not always in the same manner. In this case there are extra coefficients namely τ/ν^2 and $\tau S/\nu^2$. The filter coefficients for each scheme can be found in [34,48]. The phase speed for the Turkel–Zwas scheme is

$$\nu = \frac{f}{k}\sqrt{\tau + R_0^2 S^2}, \tag{5.6}$$

where

$$\tau = \tfrac{1}{3}(2 + \cos\, sk\ \Delta x) \tag{5.7}$$

and

$$S = \frac{\sin\, sk\ \Delta x}{s\ \Delta x}. \tag{5.8}$$

Schoenstadt concludes that Scheme A produces the greatest distortion especially at high frequencies. Other methods very accurately approximate the transfer function for high-pass filter. Scheme B overstates the amount of energy distributed into the short wave, while Scheme

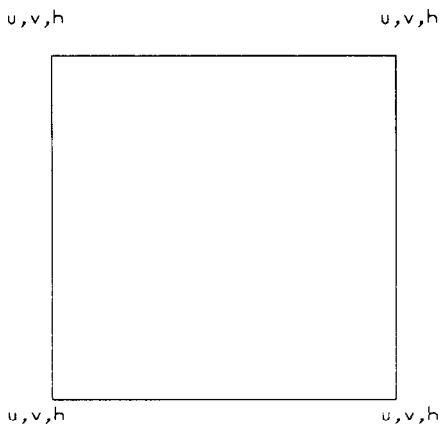

Fig. 7(a). Grid A.

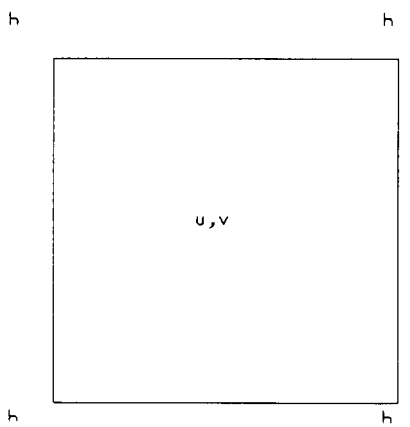

Fig. 7(b). Grid B.

C understates this. The finite-element methods appear more accurate than fourth-order finite difference. The group velocity for Schemes A, D is reversed for short waves. Based on these one-dimensional results, Scheme C is best.

6. Transfer function analysis for two-dimensional shallow water equations

The transfer function analysis initiated by Schoenstadt [48] for the one-dimensional case was extended to two dimensions in [32,33,64]. The transfer coefficients are functions of both wavenumbers k, l. The methods analyzed are the same as in the one-dimensional case. What is surprising is that the Turkel–Zwas scheme must be modified to get convergence. This modification was not enough to make the method competitive with finite-element or fourth-order C scheme. See Fig. 7 for two-dimensional arrangement of variables. The filter coeffi-

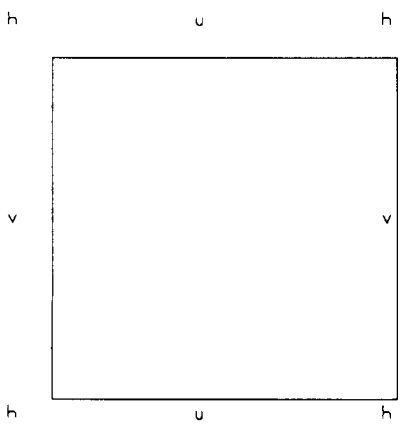

Fig. 7(c). Grid C.

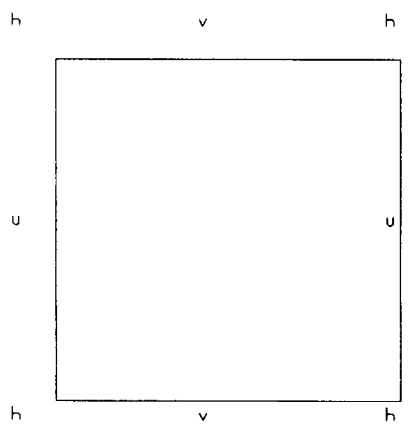

Fig. 7(d). Grid D.

Table 5

Scheme	α_x	α_y	$\beta(k, l)$
A2	1	1	$\frac{\sin kd}{d}$
B2	1	1	$\frac{\sin \frac{1}{2}kd}{\frac{1}{2}d}\cos \frac{1}{2}ld$
C2	1	$\cos \frac{1}{2}kd \cos \frac{1}{2}ld$	$\frac{\sin \frac{1}{2}kd}{\frac{1}{2}d}$
D2	1	$\cos \frac{1}{2}kd \cos \frac{1}{2}ld$	$\frac{\sin kd}{d}\cos \frac{1}{2}ld$
A4	1	1	$\frac{8 \sin kd - \sin 2kd}{6d}$
B4	1	1	$\frac{-\sin \frac{3}{2}kd + 27 \sin \frac{1}{2}kd}{12d}\cos \frac{1}{2}ld$
C4	1	$\cos \frac{1}{2}kd \cos \frac{1}{2}ld$	$\frac{-\sin \frac{3}{2}kd + 27 \sin \frac{1}{2}kd}{12d}$
D4	1	$\cos \frac{1}{2}kd \cos \frac{1}{2}ld$	$\frac{8 \sin kd - \sin 2kd}{6d}\cos \frac{1}{2}ld$
TZ	1	$\frac{1}{6}(4 + \cos ksd + \cos lsd)$	$\frac{\sin ksd}{sd}$
FET	$\frac{1}{6}(3 + \cos kd + 2 \cos \frac{1}{2}kd \cos ld)$	$\frac{1}{6}(3 + \cos kd + 2 \cos \frac{1}{2}kd \cos ld)$	$\frac{2(\sin kd + \sin \frac{1}{2}kd \cos ld)}{3d}$
FER	$\frac{1}{9}(2 + \cos kd)(2 + \cos ld)$	$\frac{1}{9}(2 + \cos kd)(2 + \cos ld)$	$\frac{1}{3}(2 + \cos ld)\frac{\sin kd}{d}$

cients for all schemes are $\alpha_y/(\alpha_x \nu)$, $\beta(k, l)/(\alpha_x \nu)$, $\beta(l, k)/(\alpha_x \nu)$, $\alpha_y \beta(k, l)/(\alpha_x^2 \nu^2)$, $\alpha_y \beta(l, k)/(\alpha_x^2 \nu^2)$ and $\beta(k, l)\beta(l, k)/(\alpha_x^2 \nu^2)$. The frequency ν is given by

$$\alpha \nu = f\sqrt{\alpha_y^2 + R_0^2(\beta^2(k, l) + \beta^2(l, k))}, \tag{6.1}$$

where α_x, α_y, β for each scheme are listed in Table 5. The only exception to the above is in the finite-element scheme on isosceles triangles (FET), in which $\beta(l, k)$ should be replaced by $(\cos \frac{1}{2}kd \sin ld)/d$.

7. Rossby wave frequencies

The hydrostatic primitive equation numerical models that are used for atmosphere and oceanographic prediction permit inertial gravity waves, Rossby waves and advective effects. The influence of a numerical method on each of these types of motion is most easily analyzed by separating the linearized prediction equations into vertical modes with an equivalent depth analysis (see, e.g., [13]). In this case the equations for each vertical mode are just the linearized shallow water equations (7.1). Arakawa and Lamb [1] analyzed inertial gravity wave motions for

grids A, B, C, D. They found that the geostrophic adjustment for grids A, D is poor and that the adjustment for grids B, C is good.

In this section we discuss the treatment of Rossby waves in vorticity-divergence shallow water formulations with various finite-element and finite-difference schemes. For comparison the finite-difference primitive equations solution for grids A, B and C are also included (see [38,64]).

7.1. Primitive form

The linearized shallow water equations on a beta plane can be written as follows:

$$\frac{\partial u}{\partial t} - fv + g\frac{\partial h}{\partial x} = 0, \tag{7.1}$$

$$\frac{\partial v}{\partial t} + fu + g\frac{\partial h}{\partial y} = 0, \tag{7.2}$$

$$\frac{\partial h}{\partial t} + H\left(\frac{\partial u}{\partial x} + \frac{\partial v}{\partial y}\right) = 0. \tag{7.3}$$

The frequency can be obtained by

$$w_F = -\frac{\beta_0 \psi}{\delta + \epsilon + \alpha\lambda^{-2}}, \tag{7.4}$$

where α, ψ, δ, ϵ depend on the method used and where β_0 is an average value of $\mathrm{d}f/\mathrm{d}y$. These parameters are listed in [38] and reproduced in Table 6.

7.2. Vorticity-divergence form

The vorticity-divergence equation set, which is obtained by differentiating (7.1) and (7.2) with respect to x and y, respectively, and combining, can be written

$$\frac{\partial \zeta}{\partial t} + fD + \beta v = 0, \tag{7.5}$$

$$\frac{\partial D}{\partial t} - f\zeta + \beta u + g\left(\frac{\partial^2 h}{\partial x^2} + \frac{\partial^2 h}{\partial y^2}\right) = 0, \tag{7.6}$$

$$\frac{\partial h}{\partial t} + HD = 0. \tag{7.7}$$

Table 6
The operators for the various numerical schemes for the shallow water equations

Scheme		Vorticity-divergence form		
		Finite elements		
Operator	Analytic	Isosceles triangles	Rectangular	Staniforth and Mitchell [55,56]
α	1	$\frac{1}{6}(3+\cos X^* + 2\cos\frac{1}{2}X\cos Y)$	$\frac{1}{9}(2+\cos X)(2+\cos Y)$	$\frac{1}{9}(2+\cos X)(2+\cos Y)$
ψ	μ	$\frac{2(\sin X + \sin\frac{1}{2}X\cos Y)}{3\,\Delta x}$	$\frac{\sin X}{\Delta x}\frac{1}{3}(2+\cos Y)$	$\frac{\sin X}{\Delta x}\frac{1}{3}(2+\cos Y)$
δ	μ^2	$\frac{\sin^2\frac{1}{2}X}{(\frac{1}{2}\Delta x)^2}$	$\frac{\sin^2\frac{1}{2}X}{(\frac{1}{2}\Delta x)^2}\frac{1}{3}(2+\cos Y)$	$\frac{\sin^2\frac{1}{2}X}{(\frac{1}{2}\Delta x)^2}\frac{1}{6}(5+\cos Y)$
ϵ	k^2	$\frac{(3+\cos X-4\cos\frac{1}{2}X\cos Y)}{2\,\Delta y^2}$	$\frac{\sin^2\frac{1}{2}Y}{(\frac{1}{2}\Delta y)^2}\frac{1}{3}(2+\cos X)$	$\frac{\sin^2\frac{1}{2}Y}{(\frac{1}{2}\Delta y)^2}\frac{1}{6}(5+\cos X)$
α'				$\frac{1}{36}(5+\cos X)(5+\cos Y)$

* $X = k\,\Delta x, Y = l\,\Delta y$.

To isolate the Rossby mode more easily we apply the quasi-geostrophic approximation to the set (7.5)–(7.7)

$$\frac{\partial\zeta}{\partial t} + f_0 D + \frac{\beta_0}{f_0} g\frac{\partial h}{\partial x} = 0, \tag{7.8}$$

$$-f_0\zeta + g\left(\frac{\partial^2 h}{\partial x^2} + \frac{\partial^2 h}{\partial y^2}\right) = 0, \tag{7.9}$$

$$\frac{\partial h}{\partial t} + HD = 0, \tag{7.10}$$

where f_0 and β_0 are evaluated at an approximate central latitude. The frequency is given as before with an appropriate value for the parameters α, ψ, δ, ϵ.

7.3. Semi-implicit fourth order

Staniforth and Mitchell [56] introduced a finite-element scheme in which the first derivatives are approximated to fourth order. The frequency in this case is given by

$$w_F = -\frac{\beta_0\psi\alpha'/\alpha}{\delta + \epsilon - \alpha'\lambda^{-2}}. \tag{7.11}$$

The parameters α, α', ψ, δ, ϵ are listed in Table 6.

Neta and Williams [38] have shown that the finite-element method based on isosceles triangles (FET) and on rectangles (FER) are as good as the method due to Staniforth and Mitchell (SM). These three methods are better than all others.

Table 6
(continued)

Vorticity-divergence form		Primitive equation form		
Finite differences		Finite differences		
Second order	Fourth order	A	B	C
1	1	1	1	$\cos^2\frac{1}{2}X \cos^2\frac{1}{2}Y$
$\frac{\sin X}{\Delta x}$	$\frac{4}{3}\frac{\sin X}{\Delta x} - \frac{1}{6}\frac{\sin 2X}{\Delta x}$	$\frac{\sin X}{\Delta x}\cos\frac{1}{2}Y$	$\frac{\sin X}{\Delta x}$	$\frac{\sin X}{\Delta x}\cos^2 Y$
$\frac{\sin^2\frac{1}{2}X}{(\frac{1}{2}\Delta x)^2}$	$\frac{\cos 2X - 16\cos X + 15}{6\,\Delta x^2}$	$\frac{\sin^2 X}{\Delta x^2}$	$\frac{\sin^2\frac{1}{2}X}{(\frac{1}{2}\Delta x)^2}\frac{1}{2}(1+\cos Y)$	$\frac{\sin^2\frac{1}{2}X}{(\frac{1}{2}\Delta x)^2}$
$\frac{\sin^2\frac{1}{2}Y}{(\frac{1}{2}\Delta y)^2}$	$\frac{\cos 2Y - 16\cos Y + 15}{6\,\Delta y^2}$	$\frac{\sin^2 Y}{\Delta y^2}$	$\frac{\sin^2\frac{1}{2}Y}{(\frac{1}{2}\Delta y)^2}\frac{1}{2}(1+\cos X)$	$\frac{\sin^2\frac{1}{2}Y}{(\frac{1}{2}\Delta y)^2}$

8. Semi-Lagrangian methods

Semi-Lagrangian methods were first proposed in [21,46], and improved recently in [59] and elsewhere. See recent review [53].

Consider the advection-diffusion equation

$$\frac{\partial\phi(x,t)}{\partial t} + v(x,t)\cdot\nabla\phi(x,t) = \nu\,\nabla^2\phi(x,t), \tag{8.1}$$

where ν is the diffusion coefficient. A semi-Lagrangian approximation may be written as [42–44]

$$\frac{\phi(x,t+\Delta t)-\phi(x-\alpha,t)}{\Delta t} = \tfrac{1}{2}\left[\nu\,\nabla^2\phi\,|_{(x,t+\Delta t)} + \nu\,\nabla^2\phi\,|_{(x-\alpha,t)}\right], \tag{8.2}$$

where

$$\alpha(x) = \Delta t\, V\left(x - \tfrac{1}{2}\alpha,\ t + \tfrac{1}{2}\Delta t\right). \tag{8.3}$$

Suppose x is a grid point of a given regular mesh. Suppose that at these mesh points we know ϕ at time t and V at time $t + \frac{1}{2}\Delta t$. A semi-Lagrangian algorithm is then the following.

(1) Solve (8.3) iteratively for $\alpha(x)$ by

$$\alpha^{(i+1)}(x) = \Delta t\, V\left(x - \tfrac{1}{2}\alpha^{(i)},\ t + \tfrac{1}{2}\Delta t\right),\quad i = 0, 1, \ldots, \tag{8.4}$$

and by an interpolation of V between mesh points.

(2) Evaluate $\nu\,\nabla^2\phi\,|_{(x,t)}$ at mesh points by finite-difference, finite-element or spectral method. Use interpolation to evaluate the right-hand side of

$$\left(\phi - \tfrac{1}{2}\nu\,\Delta t\,\nabla^2\phi\right)|_{(x,t+\Delta t)} = \left(\phi + \tfrac{1}{2}\nu\,\Delta t\,\nabla^2\phi\right)|_{(x-\alpha,t)}. \tag{8.5}$$

(3) Solve the above Helmholtz equation at mesh points (SOR, ADI, finite Fourier transform, finite elements).

(4) Repeat the steps to obtain $\phi(x, t + 2\ \Delta t)$.

Remarks. (1) Eulerian schemes suffer from serious numerical dispersion and diffusion.

(2) High-order Eulerian schemes tend to produce artificial extrema because of the unrealistic phase speeds of the high wave number.

(3) Lagrangian schemes suffer from distortion of the initial grid after a long integration (more than twelve hours).

In two dimensions it is appropriate to consider the pseudo staggering suggested in [7]. "The scheme works well with the primitive form of the equations, uses unstaggered grid but does not propagate small scale energy in the wrong direction, works well with variable resolution and as computationally efficient as staggered formulation using the primitive form of the equations."

9. Domain decomposition

One of the major developing areas in numerical analysis is parallel computation which offers the possibility of significantly faster computational speeds. Domain decomposition methods are based on subdivision of the domain into several (maybe overlapping) subdomains and solving the problem on several subdomains in parallel. The methods can be regarded as divide-and-conquer algorithms (see [65]). The interactions between the solutions on the subdomains lead to an iterative technique. When the number of subdomains is large, one can improve the convergence of this iterative procedure by using a coarse grid to obtain starting values of the solution on the interfaces. In this respect, the methods are similar to multigrid schemes. The crucial point is how to pass information from one domain to other processors. Two different approaches were followed in the literature. The first approach is based on decompositions of the domain into contiguous regions (see, e.g., [12] and references there). The second is based on having overlapping regions (Schwartz alternating method, see, e.g., [22–24] and references there).

The main difficulty of such parallel techniques is in the initial assignment of values to the interfaces between subdomains. The more accurate such values are, the faster the convergence. We have already mentioned the idea based on multigrid. There are several other possibilities to accelerate convergence (see the proceedings of four international conferences on domain decomposition [5,6,14,15]). According to Lions [24] the approach based on optimal control as followed by Glowinski et al. [16,17] is a bit faster, at least for Laplace equations.

Neta and Okamoto [35] have suggested an acceleration based on boundary elements. These two approaches for shallow water equations are now under investigation by Neta and Navon.

10. Conclusions

This paper reviewed analyses of finite-element and finite-difference schemes for the solution of the shallow water equations. The superiority of certain finite-element methods is indicated. Some recent results in parallel computations are included.

References

[1] A. Arakawa and V.R. Lamb, Computational design of the basic dynamical processes of the UCLA General Circulation Model, in: Methods Comput. Phys. 17 (Academic Press, New York, 1977) 173–265.

[2] W. Blumen, Geostrophic adjustment, *Rev. Geophys. Space Phys.* 10 (1972) 485–528.

[3] A. Cahn, An investigation of the free oscillations of a simple current system, *J. Meteorology* 2 (1945) 113–119.

[4] M.M. Cecchi, Domain decomposition method for shallow water flow problems, in: H. Niki and M. Kawahara, eds., *Proc. Internat. Conf. on Computational Methods in Flow Analysis* (Okayama Univ. of Science, Japan, 1988) 1322–1329.

[5] T.F. Chan, R. Glowinski, J. Periaux and O.B. Widlund, eds., *Proc. 2nd Internat. Symp. on Domain Decomposition Methods* (SIAM, Philadelphia, PA, 1989).

[6] T.F. Chan, R. Glowinski, J. Periaux and O.B. Widlund, eds., *Proc. 3rd Internat. Symp. on Domain Decomposition Methods for PDEs* (SIAM, Philadelphia, PA, 1989).

[7] J. Côté, S. Gravel and A. Staniforth, Improving variable-resolution finite-element semi-Lagrangian integration schemes by pseudo-staggering, *Monthly Weather Rev.* 118 (1990) 2718–2731.

[8] J. Côté and A. Staniforth, A two-time-level semi-Lagrangian semi-implicit scheme for spectral models, *Monthly Weather Rev.* 116 (1988) 2003–2012.

[9] M.P.J. Cullen and C.D. Hall, Forecasting and general circulation results from finite element models, *Quart. J. Roy. Meteorological Soc.* 105 (1979) 571–592.

[10] C.A.J. Fletcher, *Computational Galerkin Methods* (Springer, New York, 1984).

[11] M.G.G. Foreman, A two dimensional dispersion analysis of selected methods for solving the linearized shallow water equations, *J. Comput. Phys.* 56 (1984) 287–323.

[12] D. Funaro, Multidomain spectral approximation of elliptic equations, *Numer. Methods Partial Differential Equations* 2 (1986) 187–205.

[13] A.E. Gill, *Atmosphere-Ocean Dynamics* (Academic Press, New York, 1982).

[14] R. Glowinski, G.H. Golub, G.A. Meurant and J. Periaux, eds., *Proc. 1st Internat. Symp. on Domain Decomposition Methods for Partial Differential Equations* (SIAM, Philadelphia, PA, 1988).

[15] R. Glowinski, Y.A. Kuznetsov, G. Meurant, J. Periaux and O. Widlund, eds., *Proc. 4th Internat. Symp. on Domain Decomposition Methods for Partial Differential Equations* (SIAM, Philadelphia, PA, to appear).

[16] R. Glowinski and P. Le Tallec, Augmented Lagrangian interpretation of the nonoverlapping Schwarz alternating scheme, in: T.F. Chan et al., eds., *Proc. 3rd Internat. Symp. on Domain Decomposition Methods for PDEs* (SIAM, Philadelphia, PA, 1989) 224–231.

[17] R. Glowinski, Q.V. Dinh and J. Periaux, Domain decomposition methods for nonlinear problems in fluid dynamics, *Comput. Methods Appl. Mech. Engrg.* 40 (1) (1983) 27–109.

[18] G.J. Haltiner and R.T. Williams, *Numerical Prediction and Dynamic Meteorology* (Wiley, New York, 1980).

[19] R.G. Kelley and R.T. Williams, A finite element prediction model with variable element sizes, Naval Postgraduate School Report NPS-63 Wu76101, Monterey, CA, 1976.

[20] I. Kinnmark, *The Shallow-Water Wave Equations: Formulation, Analysis, and Application* (Springer, Berlin, 1985).

[21] T.N. Krishnamurti, Numerical integration of primitive equations by a quasi-Lagrangian advective scheme, *J. Appl. Met.* 1 (1962) 508–521.

[22] P.L. Lions, On the Schwarz alternating method, in: R. Glowinski et al., eds., *Proc. 1st Internat. Symp. on Domain Decomposition Methods for Partial Differential Equations* (SIAM, Philadelphia, PA, 1988) 1–42.

[23] P.L. Lions, On the Schwarz alternating method II: Stochastic interpretation and order properties, in: T.F. Chan et al., eds., *Proc. 2nd Internat. Symp. on Domain Decomposition Methods* (SIAM, Philadelphia, PA 1989) 47–70.

[24] P.L. Lions, On the Schwarz alternating method III: A variant for nonoverlapping subdomains, in: T.F. Chan et al., eds., *Proc. 3rd Internat. Symp. on Domain Decomposition Methods for PDEs* (SIAM, Philadelphia, PA, 1989) 202–223.

[25] F. Mesinger, Dependence of vorticity analogue and the Rossby wave phase speed on the choice of horizontal grid, *Sci. Math.* 10 (1979) 5–15.

[26] A.R. Mitchell and R. Wait, *The Finite Element Method in Partial Differential Equations* (Wiley, London, 1977).

[27] K.B. Monk, Studies of baroclinic flow over topography using semi-Lagrangian, semi-implicit model, Dept. Meteorology, Naval Postgraduate School, Monterey, CA, 1989.

[28] I.M. Navon, A Numerov–Galerkin technique applied to a finite-element shallow-water equations model with exact conservation of integral constraints, in: T. Kawai, ed., *Proc. 4th Internat. Symp. on Finite Element Methods in Flow Problems* (Chuo Univ., Tokyo, 1982) 75–85.
[29] I.M. Navon, A Numerov–Galerkin technique applied to a finite element shallow-water equations model with enforced conservation of integral invariants and selective lumping, *J. Comput. Phys.* 52 (1983) 313–339.
[30] I.M. Navon, A review of finite-element methods for solving the shallow-water equations, Supercomputer Computations Research Institute Report FSU-SCRI-88-49, Tallahassee, FL, 1988.
[31] I.M. Navon and H.A. Riphagen, An implicit compact fourth-order algorithm for solving the shallow-water equations in conservation-law form, *Monthly Weather Rev.* 107 (1979) 1107–1127.
[32] B. Neta, Analysis of the Turkel–Zwas scheme for the shallow-water equations, in: W.F. Ames, ed., *IMACS Trans. on Scientific Computing '88, Vols. 1.1 and 1.2: Numerical and Applied Mathematics* (Baltzer, 1989) 257–264.
[33] B. Neta and C.L. DeVito, The transfer function analysis of various schemes for the two dimensional shallow-water equations, *Comput. Math. Appl.* 16 (1988) 111–137.
[34] B. Neta and I.M. Navon, Analysis of the Turkel–Zwas scheme for the shallow-water equations, *J. Comput. Phys.* 80 (1989) 277–299.
[35] B. Neta and N. Okamoto, On domain decomposition methods for solving partial differential equations, Naval Postgraduate School Technical Report NPS-53-90-004, Monterey, CA, 1990.
[36] B. Neta and R.T. Williams, Stability and phase speed for various finite element formulations of the advection equation, *Comput. & Fluids* 14 (1986) 393–410.
[37] B. Neta and R.T. Williams, Finite elements versus finite differences for fluid flow problems, in: G.N. Pande and J. Middleton, eds., *Proc. Internat. Conf. on Numerical Methods in Engineering: Theory and Applications, II* (Martinus Nijhoff, Dordrecht, 1987) T11/1–8.
[38] B. Neta and R.T. Williams, Analysis of finite element methods for the solution of the vorticity-divergence form of the shallow water equations, in: M. Yasuhara, H. Daiguji and K. Oshima, eds., *Numerical Methods in Fluid Dynamics I, Proc. Internat. Symp. Comp. Fluid Dynamics* (Nagoya, 1989) 402–407.
[39] B. Neta, R.T. Williams and D.E. Hinsman, Studies in a shallow water fluid model with topography, in: R. Vichnevetsky and J. Vignes, eds., *Numerical Mathematics and Applications* (Elsevier, Amsterdam, 1986) 347–354.
[40] A.M. Obukhov, *Izv. Akad. Nauk SSR Ser. Geograph.-Geofiz.* 13 (4) (1949) 281.
[41] J. Pedlosky, *Geophysical Fluid Dynamics* (Springer, New York, 2nd ed., 1987).
[42] J. Pudykiewicz and A. Staniforth, Some properties and comparative performance of the semi-Lagrangian method of Robert in the solution of the advection-diffusion equation, *Atmosphere-Ocean* 22 (3) (1984) 283–308.
[43] A. Robert, A stable numerical integration scheme for the primitive meteorological equations, *Atmosphere-Ocean* 19 (1981) 35–46.
[44] A. Robert, A semi-Lagrangian and semi-implicit numerical integration scheme for the primitive meteorological equations, *J. Meteorological Soc. Japan* 60 (1982) 319–324.
[45] C.G. Rossby, On the mutual adjustment of pressure and velocity distributions in certain simple current systems, *J. Marine Research* 1 (1937–1938) 15–28; 239–263.
[46] J.S. Sawyer, A semi-Lagrangian method of solving the vorticity advection equations, *Tellus* 15 (1963) 336–342.
[47] A.L. Schoenstadt, The effect of spatial discretization on the steady-state and transient behavior of a dispersive wave equation, *J. Comput. Phys.* 23 (1977) 364–379.
[48] A.L. Schoenstadt, A transfer function analysis of numerical schemes used to simulate geostrophic adjustment, *Monthly Weather Rev.* 108 (1980) 1248–1259.
[49] H.A. Schwarz, *Gesammelte Mathematische Abhandlungen* 2 (Springer, Berlin, 1890) 133–134.
[50] G. Sewell, *Analysis of a Finite Element Method*, PDE/Protran (Springer, New York, 1985).
[51] A.N. Staniforth, The application of the finite-element method to meteorological simulations — a review, *Internat. J. Numer. Methods Fluids* 4 (1984) 1–12.
[52] A.N. Staniforth, Review: formulating efficient finite-element codes for flows in regular domains, *Internat. J. Numer. Methods Fluids* 7 (1987) 1–16.
[53] A.N. Staniforth and J. Côté, Semi-Lagrangian integration schemes for atmospheric models — a review, *Monthly Weather Rev.* 119 (1991) 2206–2223.

[54] A.N. Staniforth and R.W. Daley, A baroclinic finite-element model for regional forecasting with the primitive equations, *Monthly Weather Rev.* 107 (1979) 107–121.
[55] A.N. Staniforth and H.L. Mitchell, A semi-implicit finite-element barotropic model, *Monthly Weather Rev.* 105 (1977) 154–169.
[56] A.N. Staniforth and H.L. Mitchell, A variable resolution finite-element technique for regional forecasting with the primitive equations, *Monthly Weather Rev.* 106 (1978) 439–447.
[57] G. Strang and G.J. Fix, *An Analysis of the Finite Element Method* (Prentice-Hall, Englewood Cliffs, NJ, 1973).
[58] F.G. Stremler, *Introduction to Communication Systems* (Addison-Wesley, Reading, MA, 1977).
[59] C. Temperton and A.N. Staniforth, An efficient two-time-level semi-Lagrangian semi-implicit integration scheme, *Quart. J. Roy. Meteorological Soc.* 113 (1987) 1025–1039.
[60] V. Thomee and B. Wendroff, Convergence estimates for Galerkin methods for variable coefficient initial value problems, *SIAM J. Numer. Anal.* 11 (1974) 1059–1068.
[61] E. Turkel and G. Zwas, Explicit large time step schemes for the shallow-water equations, in: R. Vichnevetsky and R.S. Stepleman, eds., *Advances in Computer Methods for Partial Differential Equations* (IMACS, New Brunswick, NJ, 1979) 65–69.
[62] R. Vichnevetsky and J.B. Bowles, *Fourier Analysis of Numerical Approximations of Hyperbolic Equations,* SIAM Stud. Appl. Math. (SIAM, Philadelphia, PA, 1982).
[63] R. Vichnevetsky and B. Peiffer, Error waves in finite-elements and finite-difference methods for hyperbolic equations, in: R. Vichnevetsky, ed., *Advances in Computer Methods for Partial Differential Equations* (AICA, Rutgers Univ., New Brunswick, NJ, 1975).
[64] R.C. Wajsowicz, Free planetary waves in finite-difference numerical model, *J. Phys. Oceanography* 16 (1986) 773–789.
[65] O.B. Widlund, Domain decomposition algorithms and the bicentennial of the French revolution, *SIAM News* 22 (1989) 20.
[66] R.T. Williams, On the formulation of finite-element prediction models, *Monthly Weather Rev.* 109 (1981) 463–466.
[67] R.T. Williams and A.L. Schoenstadt, Formulation of efficient finite element prediction models, Naval Postgraduate School Report NPS-63-80-011, Monterey, CA, 1980.
[68] R.T. Williams and O.C. Zienkiewicz, Improved finite-element forms for the shallow-water equations, *Internat. J. Numer. Methods Fluids* 1 (1981) 81–97.
[69] F. Winninghoff, On the adjustment toward a geostrophic balance in a simple primitive equation model with application to the problem of initialization and objective analysis, Ph.D. dissertation, Univ. California, Los Angeles, 1968.
[70] O.C. Zienkiewicz, *The Finite Element Methods in Engineering Science* (McGraw-Hill, New York, 1977).